

Impurity analysis of phosphoramidites for producing oligo therapeutics

Gary Held¹ and Sven Hackbusch,² Thermo Fisher Scientific
12202 North Bartlett Avenue, Milwaukee, WI; ²355 River Oaks Pkwy, San Jose, CA 95134

Abstract

Solid-phase chemical synthesis based on phosphoramidite chemistry is one of the most widely employed approaches to synthesize oligonucleotides. With a growing number of therapeutic oligonucleotide compounds in drug development and clinical trials and the complexity of structural modifications introduced, the impurity profiling and analytical control of related starting materials have increased in importance. Here we will review the synthesis of phosphoramidites and identify sources of potential impurities. This work goes on to characterize a typical 2'-fluoro-modified phosphoramidite that is used in production of oligotherapeutics, 5'-dimethyloxytrityl-2'-fluoro-N-benzoyl-adenosine cyanoethyl phosphoramidite (5'-DMT-2'-F-A(bz)-CEP). Impurity analysis of this phosphoramidite purchased from different vendors will be presented. Identification and structure elucidation of several dozen detected impurities was done using LC-MS and will also be presented in detail.

Introduction

With the growing interest in oligonucleotide therapeutics, analysis of impurities found in phosphoramidites (amidites) has taken on increased importance. Oligonucleotide therapeutics are produced from a variety of amidites and other starting materials. Common types of amidites and other materials used in producing oligonucleotides are shown in Figure 1.

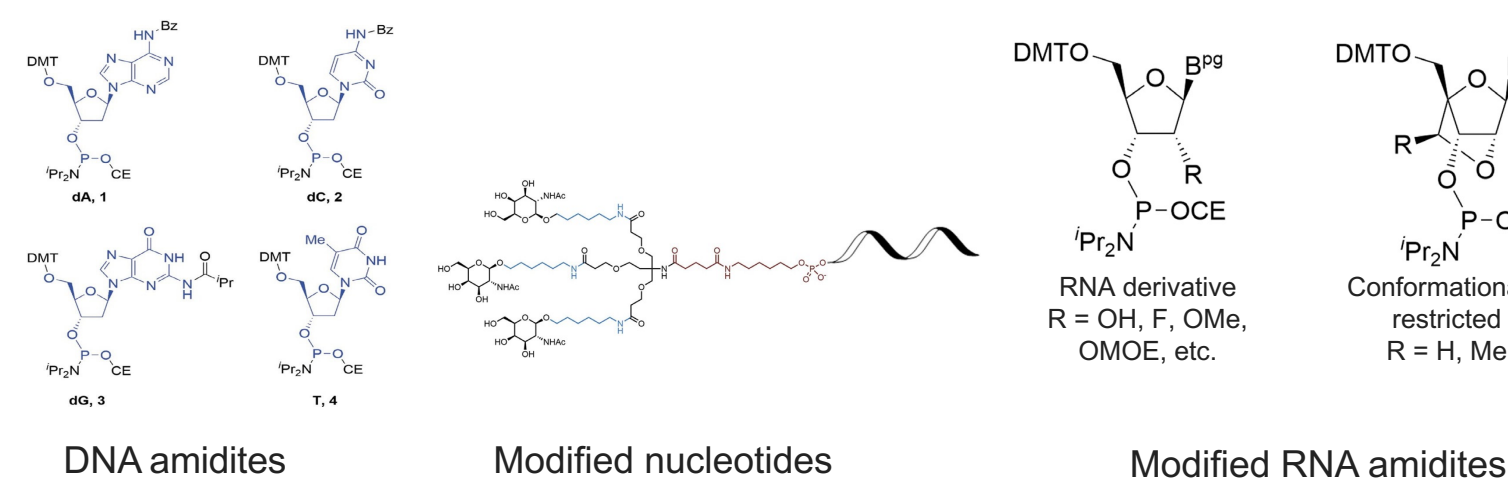


Figure 1. Common DNA and RNA amidites and modified nucleotides used for manufacturing oligonucleotide therapeutics.

Producing amidites of all types typically involves a multistep reaction process [1]. These complicated syntheses present the opportunity for generation of impurities that can ultimately end up in an amidite being used as a starting material to manufacture an oligonucleotide therapeutic. Some typical impurities can be seen in Figure 2.

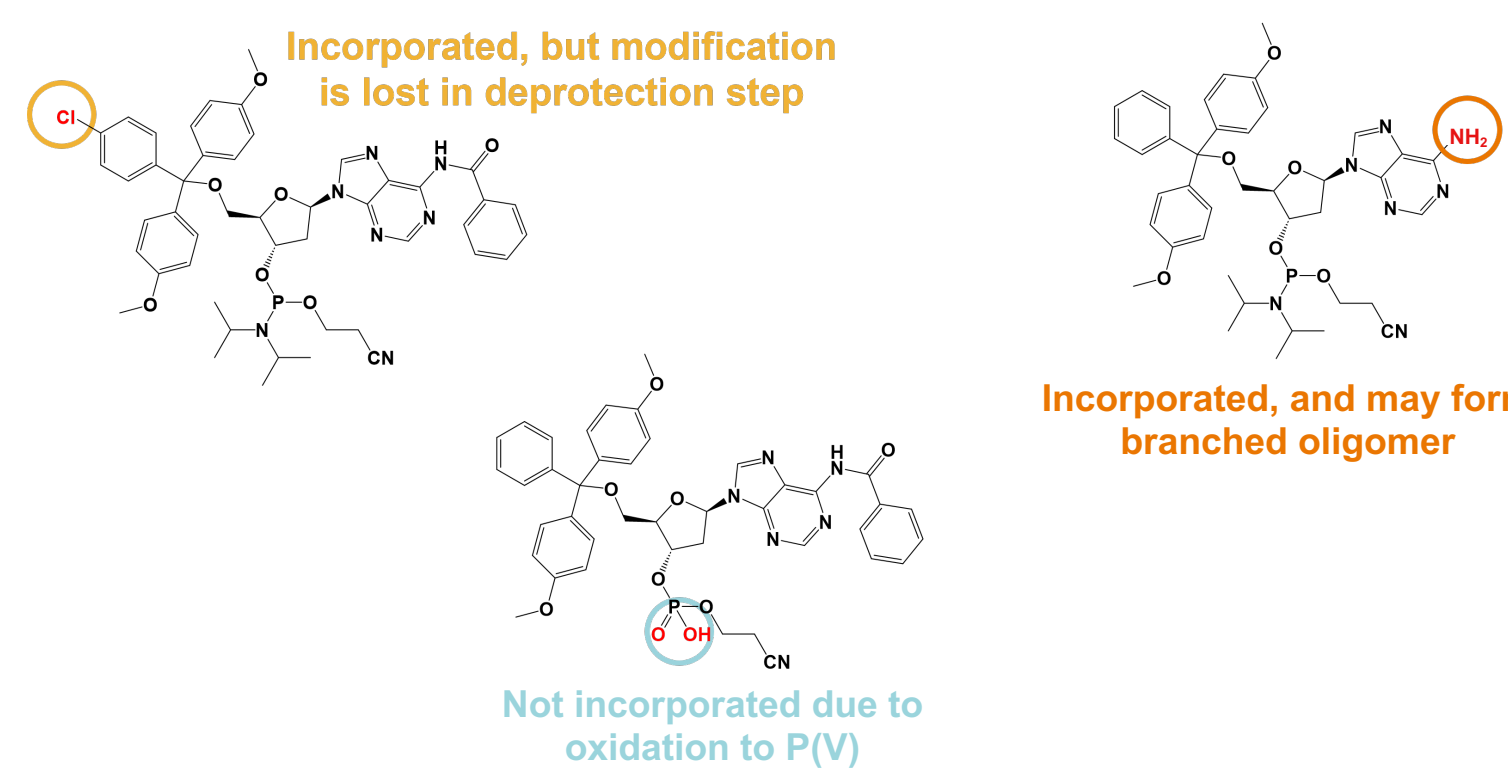


Figure 2. Examples of types of critical and noncritical impurities that can be found in amidite materials.

As such, it is essential to characterize the impurity profiles of these amidite oligonucleotide building blocks and control for them in the manufacturing process. Amidite impurities can be either critical or noncritical, depending on the type of structural modification present, and whether or not the introduced impurities can be incorporated into an oligonucleotide and if they can be removed in downstream purification steps [2].

Here we demonstrate the characterization of a phosphoramidite raw material, 5'-dimethyloxytrityl-2'-fluoro-N-benzoyl-adenosine cyanoethyl phosphoramidite (5'-DMT-2'-F-A(bz)-CEP), from different vendors and the structural elucidation of detected impurities.

Materials and methods

Sample preparation

2'-modified RNA phosphoramidites were obtained from four different vendors (referred to as A through D), with specified purities of 98% or higher. Specifically, the amidite analyzed in this work was 5'-DMT-2'-F-A(bz)-CEP.

Sample analysis by LC-MS

Impurity analysis was performed by LC-MS using a Thermo Scientific™ Vanquish™ Horizon UHPLC system equipped with a diode array detector and coupled with the Thermo Scientific™ Orbitrap Exploris™ 120 mass spectrometer. The Thermo Scientific™ Chromleon™ 7.2.10 Chromatography Data System (CDS) and Thermo Scientific™ Compound Discoverer™ 3.3 SP1 software were utilized for data analysis.

Parameter	Value
Column	Accucore C18 HPLC Column, 2.6 μm, 2.1 x 100 mm (Cat. No. 17126-102130)
Mobile phase	A: 10 mM ammonium acetate in water B: acetonitrile
Flow rate	0.4 mL/min
Column temperature	45° C (still air mode)
Autosampler temperature	6° C
Injection volume	2 μL
Needle wash solvent	50% acetonitrile
Mixer volume	35 μL (10 μL static + 25 μL capillary mixer)
Divert valve timing	Flow to waste from 0 to 1 min and 15 to 20 min
DAD settings	Wavelengths 254 nm and 200–400 nm, 5 Hz acquisition speed

Table 1. UHPLC conditions.

For separation of the raw materials, a 15-minute gradient separation as described in Table 2 using ammonium acetate buffer and acetonitrile was employed using a solid-core Thermo Scientific™ Accucore™ C18 column, which readily allowed separation of impurities from expected compounds.

Time (min)	Analytical gradient mobile phase B (%)
0.0	30
14.0	95
15.0	95
15.1	30
20.0	30

Table 2. UHPLC gradient conditions.

Results

The resulting UV and MS total ion chromatograms for the analysis of the CEP phosphoramidite are shown in Figure 3, displaying the separation of the diastereomeric product peaks. LC-MS reveals a number of impurities that are not readily detectable by UV.

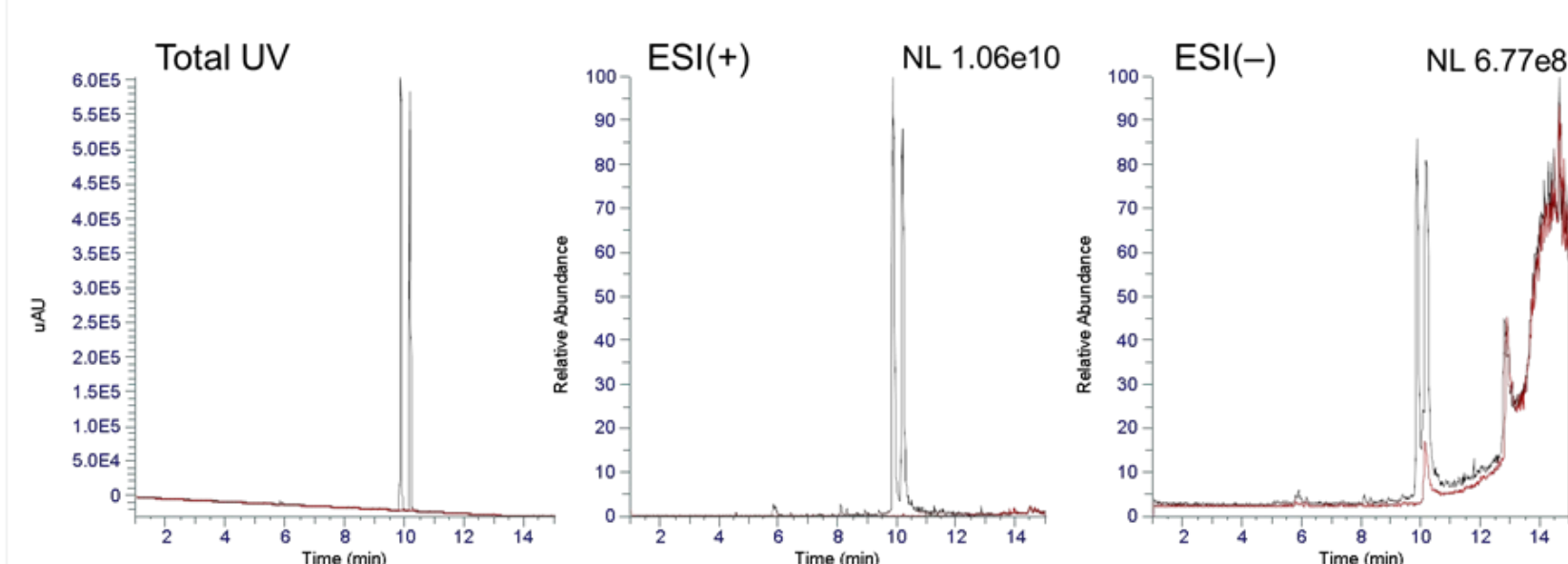


Figure 3. Representative LC-MS chromatograms of 5'-DMT-2'-F-A(bz)-CEP from vendor A at 1 mg/mL concentration (black trace), overlaid with solvent blank injection (red).

Regulatory and industry guidance typically requires analytical methods to be able to detect and characterize impurities at levels down to or below 0.1% relative to the authentic raw material [3]. To establish the sensitivity of the LC-MS method for detection of impurities at or below the level typically required, spike-in experiments were carried out using 5'-DMT-2'-F-A(bz), a potential impurity of 5'-DMT-2'-F-A(bz)-CEP resulting from loss of the cyanoethyl phosphoramidite group. Since this impurity was actually present in the phosphoramidite at detectable levels, it was instead spiked into 5'-DMT-2'-OMe-A(bz)-CEP at relative concentrations ranging from 0.001% to 0.1%, to model the case of an impurity that was not present in the unspiked sample.

The resulting UV traces and positive-mode electrospray ionization extracted ion chromatograms (ESI(+)) XICs from the different injections are shown in Figure 4. As can be seen, the impurity eluting at 5.9 min was readily detected down to a relative concentration of 0.01% using the total UV trace, while the 0.001% level was only detected in the mass spectral data.

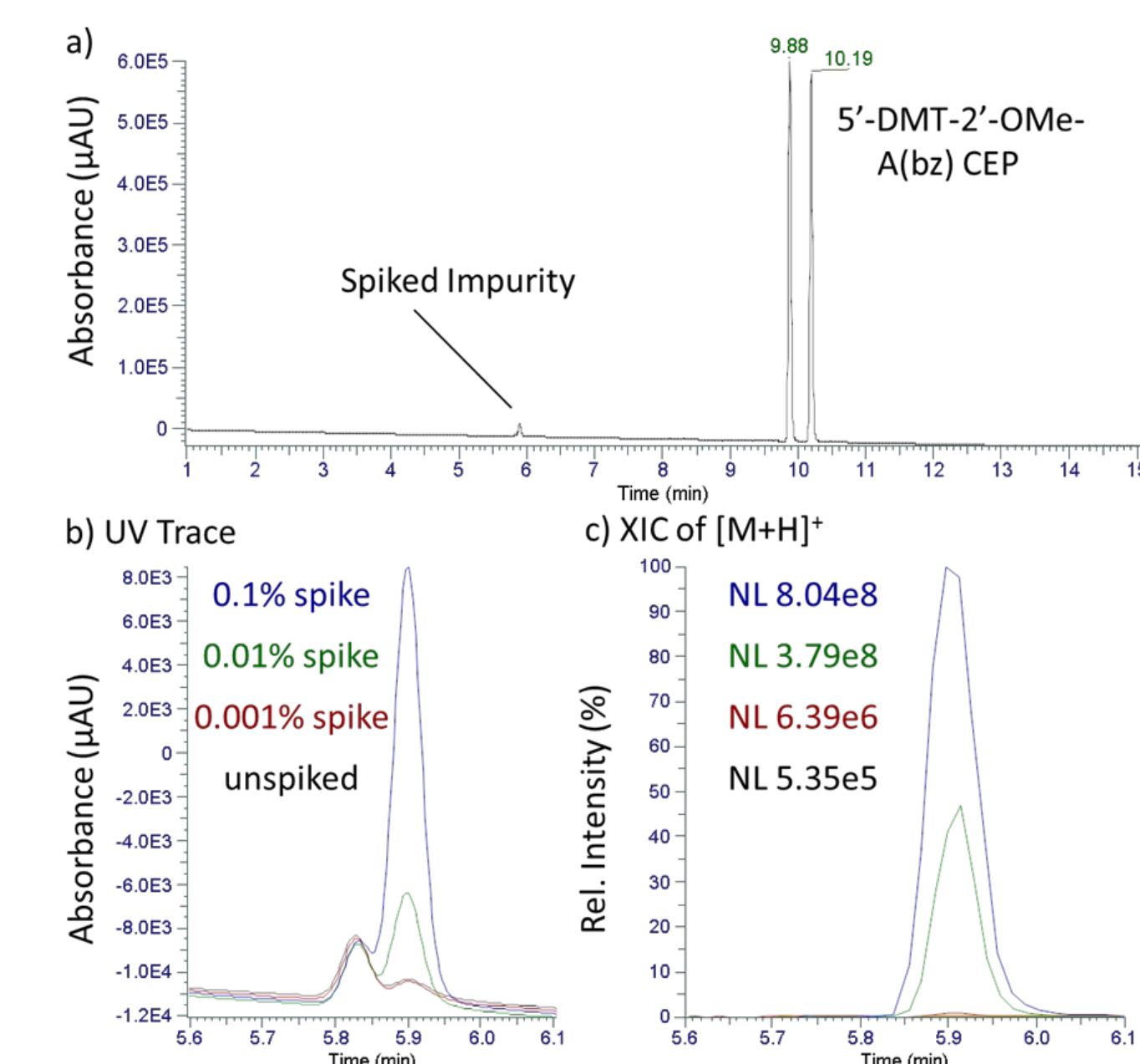


Figure 4. a) UV chromatogram showing both the spiked impurity 5'-DMT-2'-F-A(bz) and 5'-DMT-2'-OMe-A(bz)-CEP. b) UV chromatogram and c) ESI(+) XIC of the impurity.

Impurity profiling and identification

After establishing the necessary sensitivity of the method, supplies of 5'-DMT-2'-F-A(bz)-CEP obtained from four different vendors were analyzed using the established method. Based on their UV chromatograms, differences in their impurity profiles could readily be observed, as depicted in Figure 5.

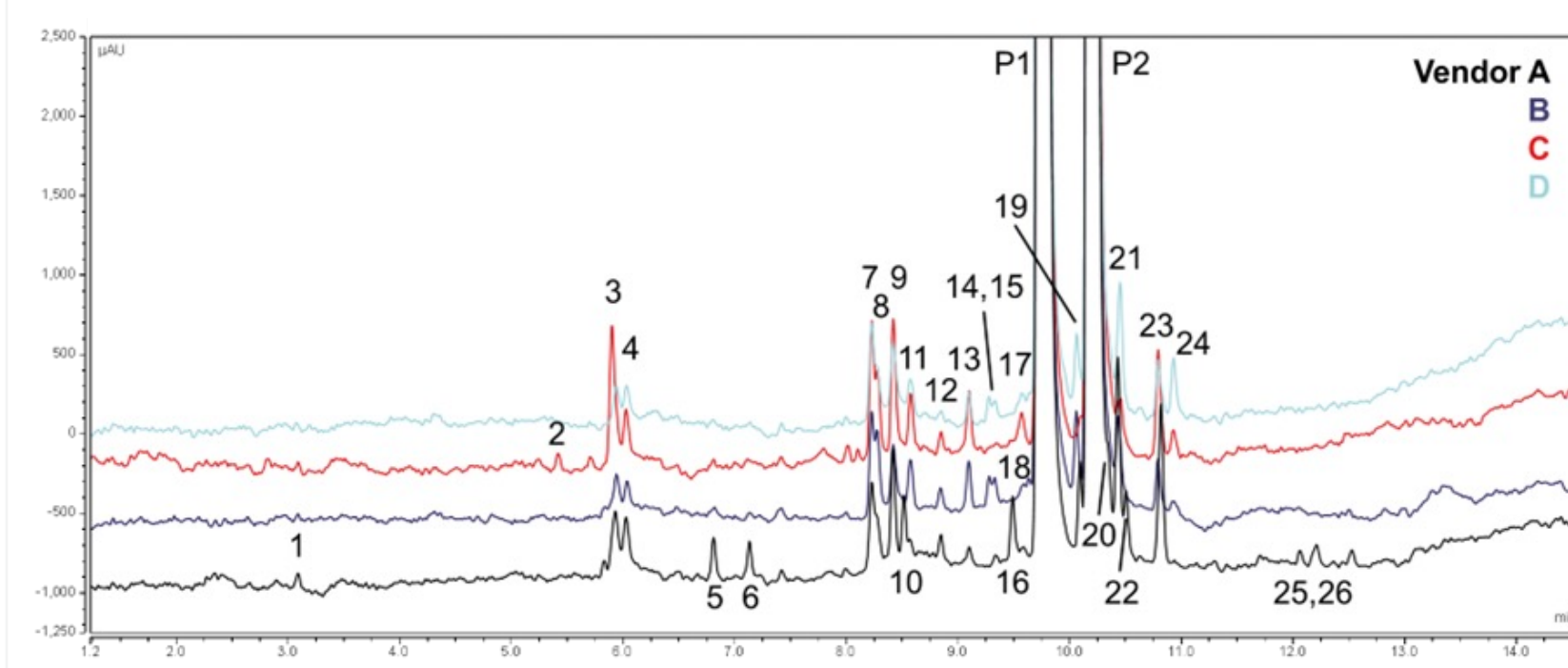
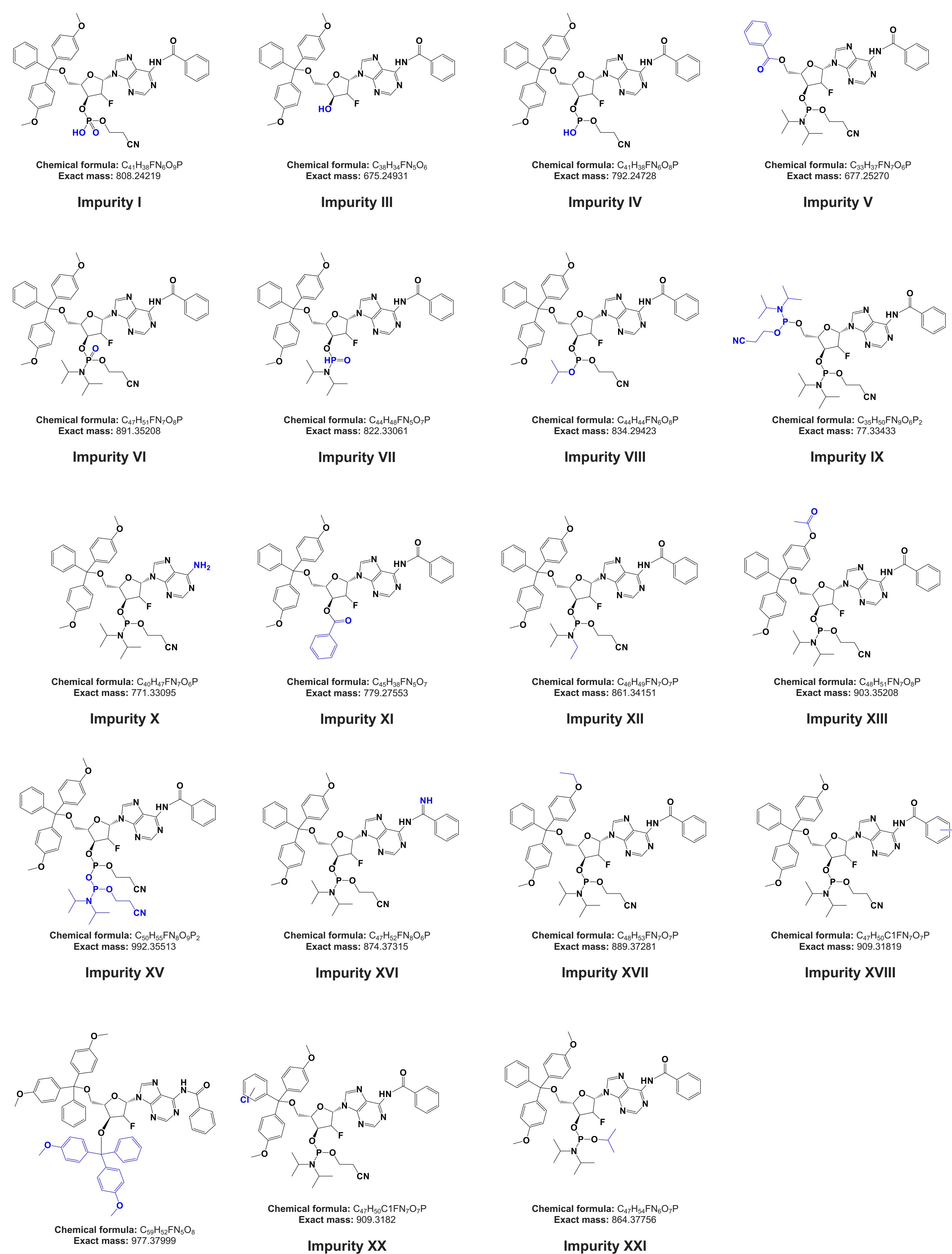


Figure 5. Zoomed-in overlay of total UV chromatograms of 5'-DMT-2'-F-A(bz)-CEP from vendors A (black), B (blue), C (red), and D (light blue), with detected impurities labeled.

The data were first processed using the qualitative workflow in the Chromleon 7.2.10 CDS to automatically detect all peaks in the total UV spectra present at or above 0.01% relative intensity. Then, both expected and unexpected (i.e., "untargeted") peak detection of the MS data were carried out using Compound Discoverer software, allowing detected UV peaks to be manually correlated to compounds detected in the MS data.

Expected compounds were generated by the software based on common transformations from the parent compound (including dealkylation, oxidation, reduction, methylation, and combinations thereof), allowing for targeted compound extraction. Meanwhile, untargeted compound detection allowed for the unbiased detection of additional compounds, particularly in cases of substitutions or additions to the parent structure, based on their relative abundance compared to a blank sample.

Based on the predicted composition and calculated transformation relative to the parent structure, candidate structures could be proposed for the impurities. Using the acquired MS² fragmentation spectra, it was possible to narrow down the possibilities and/or determine the site of transformation to allow confident annotation of the impurities as shown in Figure 6.



Impurity	MS peak (Da)	Formula	Potential Identification	Example impurity classification	% of total UV peak area by vendor			
					A	B	C	D
I	809.2422	C ₂₇ H ₃₅ F ₂ N ₃ O ₇ P	DIPA -H ₂ to P(V) species	Noncritical	0.01%	0.00%	0.00%	0.00%
II	875.2461	C ₂₇ H ₃₅ F ₂ N ₃ O ₇ P	-CEP	Noncritical	0.00%	0.00%	0.00%	0.00%
III	792.2472	C ₂₇ H ₃₅ F ₂ N ₃ O ₇ P	DIPA -OH	Noncritical	0.07%	0.00%	0.07%	0.00%
IV	877.2525	C ₂₇ H ₃₅ F ₂ N ₃ O ₇ P	DMT -H ₂	Noncritical	0.00%	0.00%	0.00%	0.00%
V	891.2518	C ₂₇ H ₃₅ F ₂ N ₃ O ₇ P	Oxidation to P(V) species	Noncritical	0.00%	0.10%	0.13%	0.13%
VI	822.3306	C ₂₇ H ₃₅ F ₂ N ₃ O ₇ P	H ₂ O phosphate + loss of cyanoethyl group	Noncritical	0.01%	0.01%	0.04%	0.00%
VII	834.2944	C ₂₇ H ₃₅ F ₂ N ₃ O ₇ P	Substitution of DIPA with P(OH)	Noncritical	0.00%	0.00%	0.00%	0.00%
VIII	773.2341	C ₂₇ H ₃₅ F ₂ N ₃ O ₇ P	-DMT -CEP	Critical	0.01%	0.00%	0.00%	0.00%
IX	773.2307	C ₂₇ H ₃₅ F ₂ N ₃ O ₇ P	-H ₂	Critical	0.01%	0.00%	0.00%	0.00%
X	779.2733	C ₂₇ H ₃₅ F ₂ N ₃ O ₇ P	-CEP -H ₂	Noncritical	0.01%	0.01%	0.01%	0.00%
XI	861.3414	C ₂₇ H ₃₅ F ₂ N ₃ O ₇ P	Demethylation on CEP	Noncritical	0.00%	0.00%	0.00%	0.01%
XII	803.3518	C ₂₇ H ₃₅ F ₂ N ₃ O ₇ P	Acyloxy-methyl substitution on DMT	Noncritical	0.00%	0.01%	0.00%	0.01%
XIII	862.3551	C ₂₇ H ₃₅ F ₂ N ₃ O ₇ P	DIPA -CEP	Noncritical	0.00%	0.00%	0.00%	0.00%
XIV	874.3732	C ₂₇ H ₃₅ F ₂ N ₃ O ₇ P	-O -NH ₂ on bz	Noncritical	0.00%	0.00%	0.04%	0.00%
XV	889.3721	C ₂₇ H ₃₅ F ₂ N ₃ O ₇ P	Methylation on DMT	Noncritical	0.00%	0.00%	0.00%	0.00%
XVI	909.3177	C ₂₇ H ₃₅ F ₂ N ₃ O ₇ P	Oxidation on bz	Noncritical	0.12%	0.01%	0.00%	0.00%
XVII	977.3799	C ₂₇ H ₃₅ F ₂ N ₃ O ₇ P	-CEP -DMT	Noncritical	0.02%	0.01%	0.00%	0.00%
XVIII	893.3177	C ₂₇ H ₃₅ F ₂ N ₃ O ₇ P	Oxidation on DMT	Noncritical	0.00%	0.01%	0.01%	0.00%
XIX	864.3776	C ₂₇ H ₃₅ F ₂ N ₃ O ₇ P	-CN -O ₂ -H ₂	Critical	0.00%	0.00%	0.00%	0.00%
XX	873.3311	C ₂₇ H ₃₅ F ₂ N ₃ O ₇ P	5'-DMT-2'-F-A(bz)-CEP	Critical	99.33%	99.61%	99.64%	99.61%
Critical impurity level					0.00%	0.00%	0.01%	0.00%

Figure 6. Summary of detected impurities in 5'-DMT-2'-F-A(bz)-CEP and relative amounts detected in the materials from the different vendors (A–D).

Conclusions

With the increased interest in therapeutic oligonucleotides, having confidence in impurity characterization of phosphoramidite building blocks has gained importance. Here we highlight the need for highly sensitive, high-quality MS data to facilitate confident identification of phosphoramidite impurities and their profiling across different suppliers' materials.

- The analytical method's suitability for sensitive detection of trace impurities at levels of 0.01% and lower was demonstrated using a spike-in experiment.
- Differences in the impurity profiles of 5'-DMT-2'-F-A(bz)-CEP from different vendors were readily determined, and while all investigated samples showed high purity exceeding the respective vendors' specifications, different levels of impurities that are important to control for in the manufacturing of therapeutic oligonucleotides could be observed.

References

- Roy S, Caruthers M (2013) Synthesis of DNA/RNA and their analogs via phosphoramidite and H-phosphonate chemistries. *Molecules* 18:14268–14284. doi: [10.3390/molecules181114268](https://doi.org/10.3390/molecules181114268)
- Kiesman WF et al. (2021) Perspectives on the designation of oligonucleotide starting materials. *Nucleic Acid Therapeutics* 31:93–113. doi: [10.1089/nat.2020.0909](https://doi.org/10.1089/nat.2020.0909)
- ICH, Q3A(R) Impurities in new drug substances (February 2003) and others.